

Groundbreaking research

Journal of
Cerebral Blood Flow
& Metabolism

Journal of Cerebral Blood Flow & Metabolism (2000) **20**, 280–289; doi:
10.1097/00004647-200002000-00009

Oxygen Dependency of Cerebral Oxidative Phosphorylation in Newborn Piglets

Financial assistance provided by Hamamatsu Photonics KK.

Roger Springett, Marzena Wylezinska*, Ernest B Cady*, Mark Cope and David T Delpy

1. Department of Medical Physics and Bioengineering, University College London, London, England
2. *University College Hospitals NHS Trust, London, England

Correspondence: Roger Springett, Department of Medical Physics and Bioengineering, University College London, Shropshire House, 11-20 Capper St., London, WC1E 6JA, U.K.

Received 14 July 1999; Revised 22 October 1999; Accepted 28 October 1999.

Abstract

Changes in hemoglobin oxygenation and oxidation state of the Cu_A centre of cytochrome oxidase were measured with full spectral near infrared spectroscopy simultaneously with phosphorus metabolites using nuclear magnetic resonance ³¹P spectroscopy at high time resolution (10 seconds) during transient anoxia (F_iO₂ = 0.0 for 105 seconds) in the newborn piglet brain. During the onset of anoxia, there was no change in either phosphocreatine (PCr) concentration or the oxidation state of the Cu_A centre of cytochrome oxidase until there was a substantial fall in cerebral hemoglobin oxygenation, at which point the Cu_A centre reduced simultaneously with the decline in PCr. At a later time during the anoxia, intracellular pH decreased rapidly, consistent with a fall in cerebral metabolic rate for O₂ and reduced flux through the tricarboxylic acid cycle. The simultaneous reduction of Cu_A and decline in PCr can be explained in terms of the effects of the falling mitochondrial electrochemical potential. From these observations, it is concluded that, at normoxia, oxidative phosphorylation and the oxidation state of the components of the electron transport chain are independent of cerebral oxygenation and

that the reduction in the Cu_A signal occurs when oxygen tension limits the capacity of oxidative phosphorylation to maintain the phosphorylation potential.

Keywords:

Near infrared spectroscopy, ³¹P nuclear magnetic resonance spectroscopy, Cytochrome oxidase, Hypoxia

Abbreviations:

CBF, cerebral blood flow; CMRO₂, cerebral metabolic rate for oxygen; FID, free induction delay; Hb, deoxyhemoglobin; HbO₂, oxyhemoglobin; HbT, total hemoglobin; NIRS, near infrared spectroscopy; NMRS, nuclear magnetic resonance spectroscopy; PCr, phosphocreatine

In the adult rat brain, oxygen consumption is independent of arterial oxygen tension until arterial oxygen tension falls below ~25 mm Hg ([Siesjö, 1978](#)). Although the fall in oxygen delivery is partly compensated during hypoxaemia by an increase in cerebral blood flow (CBF), many authors have suggested that the redox components of the electron transport chain become more reduced as part of a mechanism to maintain oxygen consumption and ATP synthesis. However, supporting evidence relies on the use of optical techniques, for example, NADH fluorescence techniques to measure mitochondrial NADH/NAD⁺ redox changes, visible spectroscopy to measure redox changes of the haem a centre of cytochrome oxidase, and near infrared spectroscopy (NIRS) to measure changes in the redox state of the Cu_A centre of cytochrome oxidase. In general, the signals from these techniques show a continuous redox reduction from hyperoxia to hypoxia [see, e.g., [Gyulai et al. \(1988\)](#); NADH fluorescence), [Kreisman et al. \(1981\)](#); visible spectroscopy), and [Hampson et al. \(1990\)](#); NIRS)], although there are exceptions ([Hoshi et al., 1997](#); [Cooper et al., 1994](#)). However, all optical techniques are susceptible to interference by hemoglobin, which does show continuous changes in oxygenation and total concentration between hyperoxia and hypoxia.

Whether the redox state of the electron transport chain is dependent on cerebral oxygenation at normoxia is critical to the understanding of the coupling of blood flow and metabolism during functional activation. Based on the assumption that mitochondrial oxygen tension is either constant or very low, it has been predicted ([Buxton and Frank, 1997](#)) that large increases in CBF are necessary to accommodate small increases in cerebral metabolic rate for O₂ (CMRO₂), as observed in positron emission tomography functional activation studies ([Fox et al., 1988](#)). However, if the oxygen tension at the mitochondria is substantially above a critical level, then increased oxygen consumption by the mitochondria can drive the mitochondrial oxygen tension lower and increase the rate of oxygen diffusion from capillary to mitochondria without the need for large increases in CBF.

In vitro work on mitochondrial suspensions has shown that in coupled mitochondria, the electron transport chain from NADH to cytochrome c operates reversibly and at

equilibrium ([Erecinska et al., 1974](#); [Forman and Wilson, 1982](#); [Nishiki et al., 1978](#); [Greenbaum and Wilson, 1991](#)). Within the framework of the chemiosmotic theory of oxidative phosphorylation, this can be interpreted to mean that the free energy released when electrons are passed from NADH to cytochrome c is equal to the free energy required to pump protons against the electrochemical gradient, that is, [Equation \(1\)](#) where n_p is the number of protons pumped by complex I and complex III per electron transferred, $\Delta\mu_{H^+}$ is the electrochemical potential defined as the free energy change when protons are translocated across the mitochondrial membrane from cytosol to matrix, F is the Faraday constant, and E_{NADH} and E_{cytc} are the redox potentials of NAD and cytochrome c. Furthermore, the mitochondrial electrochemical potential has been shown to be in equilibrium with the cytosolic phosphorylation potential via the mitochondrial F_1F_0 -ATP synthase ([Wang and Oster, 1998](#)), the adenine nucleotide translocase, and phosphate translocase ([Forman and Wilson, 1983](#)), that is, [Equation \(2\)](#) where n_s is the number of protons translocated across the mitochondrial membrane per ATP synthesised and ΔG_p is the cytosolic phosphorylation potential, defined as the free energy change on hydrolysis of ATP. Thus, changes in the phosphorylation potential can be used to infer changes in the redox state of the electron transport chain: As the phosphorylation potential becomes less negative, the electrochemical potential becomes less negative ([Eq. 2](#)) and cytochrome c becomes more reduced with respect to the $NAD^+/NADH$ redox couple ([Eq. 1](#)).

$$n_p \Delta\mu_{H^+} = F(E_{NADH} - E_{cytc})$$

$$n_s \Delta\mu_{H^+} = \Delta G_p$$

In vivo phosphorus (^{31}P) nuclear magnetic resonance spectroscopy (NMRS) is an established noninvasive technique for measuring the intracellular concentrations of ATP, inorganic phosphate (P_i), and phosphocreatine (PCr). Although the concentration of free ADP is too low to be measured directly, the cytosolic phosphorylation potential can be calculated, assuming that the creatine kinase reaction remains in equilibrium ([Siesjö, 1978](#)). In addition, intracellular pH (pH_i) can be calculated from the chemical shift between the PCr and P_i ([Moon and Richards, 1973](#)).

Near infrared spectroscopy is a noninvasive technique that has the potential to measure changes in the concentration of oxyhemoglobin (HbO_2) and deoxyhemoglobin (Hb) and the oxidation state of the Cu_A centre of cytochrome oxidase (Cu_A). However, accurate measurement of the change in the Cu_A oxidation state is error-prone because it represents a small component of the signal compared with hemoglobin and the oxidised cytochrome spectrum is similar in shape to that of HbO_2 . For this study, a full spectral charge-coupled device (CCD) spectrometer system was used, which has been shown by modelling to be more precise in separating the Cu_A signal from the hemoglobin signals than two- or four-wavelength systems ([Matcher et al., 1995](#)). The robustness of the Cu_A signal from this system and in this model has been partially validated using cyanide ([Cooper et al., 1999](#)). Use of a full spectral system has the added advantage that the optical path length can also

be measured from the second differential feature of water ([Matcher et al., 1994](#)) and so changes in the concentration of HbO₂ and Hb and Cu_A oxidation state can be expressed in units of concentration ($\mu\text{mol/L}$).

The aim of this study was to determine whether, at normoxia, the redox state of the electron transport chain is dependent on cerebral oxygenation. This was achieved by simultaneously measuring phosphorus metabolites using NMRS and NIRS parameters with a high temporal resolution during brief anoxia ($F_{iO_2} = 0.0$ for 105 seconds); brief anoxia leads to rapid cerebral desaturation, a reduction in the Cu_A centre of cytochrome oxidase, and a fall in the phosphorylation potential. By careful registration between the NIRS and NMRS signals, it was possible to determine the sequence of events that led to energy failure.

Previous comparisons between ³¹P metabolites and electron transport chain redox state ([Gyulai et al., 1988](#); [Tsuji et al., 1995](#); [Matsumoto et al., 1996](#)) have correlated NMRS parameters with redox state at different arterial PO₂ values. However, maintaining PaO₂ at low values for periods of many minutes necessary to obtain phosphorus spectra can lead to circulatory failure, resulting in partial cerebral ischaemia, a more profound cellular acidosis, and severe energy failure [cf. data of [Tsuji et al. \(1995\)](#) and [Matsumoto et al. \(1996\)](#) with the data presented here]. Such changes can lead to cellular oedema and a change in the tissue-scattering coefficient that are not accounted for by the NIRS algorithm used to separate attenuation changes into chromophore concentration changes and that may lead to spurious changes in the redox signal. This complicates the data analysis compared with the brief anoxia used here and, in particular, the use of a neonatal piglet model, in which the heart is more resistant to transient hypoxia and blood pressure and hence cerebral perfusion is maintained.

To obtain high-quality NMR spectra with the required time resolution, it was necessary to perform the brief anoxia six times in each piglet and to sum the NMR spectra for each time point of the six anoxias. For this process to be valid, it is necessary to show that the anoxia is highly reproducible.

[Top of page](#)

METHODS

Six piglets, born at term but less than 24 hours old and weighing 1.72 ± 0.14 (SD) kg, were sedated with midazolam and anaesthetised with 2% isoflurane. A tracheotomy was performed, and the piglets were artificially ventilated with an intermittent positive pressure ventilator using an oxygen and nitrogen gas mixture. The inspired oxygen fraction was set to 0.4, and the inspiratory pressure and the respiration rate set to give an arterial CO₂ level (PaCO₂) of between 30 and 40 mm Hg.

Cannulae were sited in the umbilical vein and artery for infusion of fluids and for collecting blood samples to perform blood gas analysis (ABL505; Radiometer, Copenhagen, Denmark), respectively. To prevent hypoglycaemia, 10% glucose solution

was infused intravenously at 2 mL/h and arterial blood glucose and lactate were measured periodically (2300 STAT Plus; YSI, Yellow Springs, OH, U.S.A.). Heart rate and mean arterial blood pressure were monitored from the umbilical arterial line using a strain gauge pressure transducer. Rectal temperature was maintained at 38.5°C using a heated water mattress.

The piglets were placed in a custom-made pod in the bore of a 7 T Bruker Avance spectrometer (Karlsruhe, Germany) with a 21-cm bore and a ^{31}P frequency of 121 MHz. The head was fixed in a stereotaxic frame that also held a 25-mm-diameter double-tuned (^{31}P and protons) inductively coupled surface coil against the intact scalp over the parietal lobes and two end-on optodes 35 mm apart symmetrically about the midline ~1 cm posterior to the eyes. In this configuration, the NIR optodes and ^{31}P surface coil were expected to probe approximately the same volume of tissue. The optodes were surrounded by NIR-opaque sponges (~1 cm square), pressed firmly against the head, and NIR-opaque polyvinylchloride tape was used to shield the cranium between and around the optodes and beneath the surface coil. The use of the sponges and tape ensured that light emerging near the transmit optodes did not reenter the head near the receive optode and interfere with the attenuation measurement.

The homogeneity of the static magnetic field was optimised by monitoring the signal of brain water protons, and a half-height width of <30 Hz was normally obtained. The pulse sequence consisted of a Dante pulse train ([Morris and Freeman, 1978](#)) of 500 10-microsecond pulses with a 200-microsecond repetition time to reduce signals from bone and phospholipids, followed by a square acquisition pulse (180° flip angle at the centre of the coil). The repetition time was 2 seconds; 4,096 quadrature points were collected with a spectral width of 14 kHz; and four free induction decays (FIDs) were averaged, giving a spectrum with a temporal resolution of 10 seconds. Six ^{31}P spectra (24 FIDs) from corresponding time points on the repeated brief anoxias were summed, exponentially weighted with an 8-Hz filter, Fourier transformed, and phase corrected. Relative concentrations of phosphorus metabolites were obtained by fitting Lorentzian peaks to the real component of the phosphorus spectra using a nonlinear iterative curve-fitting method and a quartic background; peak height and position were allowed to vary, whereas peak width was determined from baseline spectra and fixed during the fitting process because no changes were observed in the line width of the resonance peaks.

The high temporal resolution precluded the acquisition of fully relaxed ^{31}P spectra so that relative concentrations of different metabolites could not be compared, although the relative concentration of each metabolite remained proportional to the peak area, assuming the relaxation time did not change over the period of anoxia (this assumption was supported by the stability of the ATP peak). Therefore, concentrations of ATP, PCr, and P_i were expressed as the peak height of the ATP- β , PCr, and P_i peaks relative to baseline PCr peak height; peak height is proportional to peak area at constant peak width.

Light from a stabilised tungsten halogen light source was filtered with a 610-nm long-pass filter and transmitted to the piglet head with a glass optic fibre bundle (3.3-mm diameter). Transmitted light was collected with a second fibre bundle and focused onto

the slits of a 0.27-m spectrograph (270M; Instruments SA, Lonjumeau, France) equipped with a 300-g/mm grating blazed at 1,000 nm. The NIR spectra between 650 and 980 nm were collected contiguously every second on a charge-coupled device detector (Wright Instruments, Enfield, London, U.K.) with the shutter held open. The pixel bandwidth was 0.32 nm, and the slits set to give a signal of $\approx 100,000$ electrons per digital conversion at 800 nm; spectral resolution was between 2.5 and 3.7 nm.

Changes in HbO₂, Hb, and Cu_A were determined by fitting changes in the attenuation spectra between 780 and 900 nm to *in vitro* absorption spectra of HbO₂, Hb, and Cu_A that had been corrected for the wavelength dependence of path length ([Essenpreis et al., 1993](#)). The optical path length at the 840-nm water absorption feature was obtained by fitting the second differential of the attenuation spectra to the second differential of water and Hb absorption spectra between 800 and 880 nm. The path length was converted to units of centimetres by assuming an average cerebral water content of 85%. Changes in HbO₂, Hb, and Cu_A were converted to units of millimoles per litre using the 840-nm water path length derived from baseline spectra. Total hemoglobin (HbT) is the sum of HbO₂ and Hb.

After surgery and once the piglet had been positioned in the magnet, the isoflurane was reduced to 1.5 to 1.8% and the piglet allowed to stabilise over a period of at least 1 hour, during which NIR spectra were recorded. The experimental protocol consisted of six transient anoxias in which the inspired oxygen fraction was reduced from 0.4 to 0.0 for 105 seconds. Transient anoxias were performed at intervals of 20 minutes. The NIRS and ³¹P data were collected continuously throughout, and blood samples for gas and glucose/lactate analysis were collected 2 minutes before each anoxia.

The NIR attenuation spectra were collected contiguously every second throughout the study, and heart rate, blood pressure, and rectal temperature were logged simultaneously by the NIRS software. The gas mixture fed to the piglets was controlled using a computerised gas blender ([Elwell et al., 1994](#)) and was switched synchronously with the NIRS data collection. The ³¹P spectra were collected contiguously every 10 seconds asynchronously with respect to the NIRS data collection, and the beginning of each spectrum was logged by the NIR software. At the end of the study, the attenuation spectra, NIRS parameters, and logged physiological parameters were averaged over the period of each ³¹P spectrum to give a complete data set of six anoxias with a temporal resolution of 10 seconds for each piglet. The mean and SD of the NIRS data and logged physical parameters were calculated over the six anoxias, and the NMR FID data were summed to provide sufficient signal-to-noise ratio. To time-normalise each anoxia for averaging, time zero was chosen as the first data point at which HbO₂ fell below baseline during the onset of anoxia. Although gas switching was not synchronized to NMRS data collection, this method maintains temporal accuracy to ± 5 seconds. The time-normalisation data point is marked as time zero in the figures.

Analysis of variance was used to compare repeated measurements, and all data are presented as mean \pm SD ($n = 6$ animals). The significance of changes was determined using a paired Student *t* test; the criterion for significance was $P < 0.05$.

[Top of page](#)

RESULTS

Before the first anoxia and calculated (mean \pm SD) over the six piglets, mean arterial blood pressure was 49.7 ± 5.1 mm Hg, heart rate was 182 ± 16 beats/min, arterial pH was 7.54 ± 0.01 , arterial PO₂ was 145 ± 23 mm Hg, and arterial PCO₂ was 35.6 ± 3.6 mm Hg. These values are all in the normal physiological range for the newborn piglet and did not change significantly between baseline periods before each anoxia. The baseline values of mean arterial blood pressure are shown in [Table 1](#) to demonstrate the degree of cardiovascular stability. Rectal temperature remained in the range of 38.5 to 38.7°C, which is normal for a newborn piglet, but the precision of the temperature probe (0.1°C) precluded statistical analysis. Each anoxia increased arterial plasma lactate significantly from 1.5 mmol/L before the first anoxia to 2.5 mmol/L before the last and increased arterial plasma glucose significantly from 5.0 ± 0.9 mmol/L before the first anoxia to 5.6 ± 1.3 mmol/L before the last anoxia (see [Table 1](#)).

[Table 1 - Physiologic, NIR, and ³¹P NMRS variables, expressed as mean \$\pm\$ SD \(n = 6\), measured 2 minutes before each anoxia.](#)



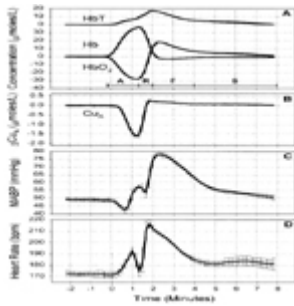
[Full table](#)

The baseline values for the NMRS and NIRS parameters before each anoxia are shown in [Table 1](#). The NMR parameters were obtained by averaging six phosphorus spectra (24 FIDs) in the baseline period between 2.5 and 1.5 minutes before each anoxia. In general, there were no significant changes in these parameters before each anoxia except for HbO₂, which showed a continuous small decrease that obtained significance before the fourth anoxia, and P_i, which showed small significant decreases before the second and third anoxias. None of these changes were significant at the $P = 0.01$ level.

[Figure 1](#) shows changes in HbO₂, Hb, HbT, Cu_A, mean arterial blood pressure, and heart rate of a typical piglet expressed as mean and SD averaged over the six anoxias (see Methods). The period of anoxia is marked as A on [Fig. 1](#). The reduction in arterial saturation leads to a fall in HbO₂ and rise in Hb starting at time zero in the figure. From the beginning of anoxia, oxygen tension at the cellular level would have been falling, but it was not until HbO₂ had fallen substantially that there was a reduction in the Cu_A signal. The increase in HbT is consistent with an increase in CBF that had been triggered by the hypoxaemia. Reoxygenation, marked as R in [Fig. 1](#), was first observed at 90 seconds, and there was simultaneous cerebral reoxygenation and oxidation of the Cu_A centre of cytochrome oxidase. Arterial saturation rapidly returned to normal levels, but there was

an increase in HbO₂ and a decrease in Hb compared with baseline values, consistent with an increase in CBF. The HbT reached a maximum at ≈120 seconds and HbO₂ at ≈150 seconds, and then HbT, HbO₂, and Hb returned to baseline values over the subsequent 8 minutes.

Figure 1.



Changes in total hemoglobin (HbT), oxyhemoglobin (HbO₂), and deoxyhemoglobin (Hb) (A), oxidation state of the Cu_A centre of cytochrome oxidase (B), mean arterial blood pressure (C), and heart rate (D) expressed as mean and SD calculated from the six anoxias from a single piglet. In the top panel, HbT has been offset for clarity.

[Full figure and legend \(259K\)](#)

The apparent discrepancy between the period of F_iO₂ = 0.0 (105 seconds) and the period of the anoxia observed in the head (90 seconds) is the result of gas mixing and transit time in the ventilation tubing and not an artefact of the averaging procedure. The same period is observed in the data before averaging.

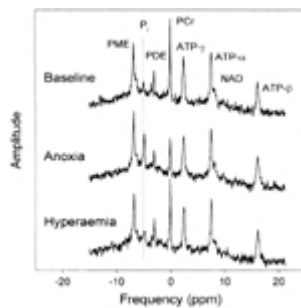
The hyperaemic period after reoxygenation can be loosely split into two phases: the fast phase (marked as F on [Fig. 1](#)), which lasted from 2 to ≈4 minutes after anoxia, in which the HbT and Cu_A signals rapidly returned towards baseline, and the slow phase (marked as S on [Fig. 1](#)), which covered the period 4 to 8 minutes, in which the HbT slowly returned to baseline.

The lower panels of [Fig. 1](#) show mean arterial blood pressure and heart rate during the anoxia. The baseline heart rate in this piglet was 171 ±3 beats/min and increased at the onset of anoxia to 193 ±3 beats/min before falling at the depth of the anoxia to 174 ±4 beats/min. At the onset of anoxia, mean arterial blood pressure fell from a baseline value of 48.7 ±1.3 to 42.5 ±1.8 mm Hg and then rose to 57.5 ±1.2 mm Hg before falling to 53.4 ±2.9 mm Hg during the period of bradycardia. On reoxygenation, there was a rapid rise in mean arterial blood pressure and heart rate, which returned to baseline with a similar biphasic pattern as the hemoglobin parameters but with a slightly longer time course.

The error bars in [Fig. 1](#) are representative of the reproducibility of the transient anoxia in all the piglets studied. The larger error bars during desaturation and reoxygenation are probably the result of slight timing differences between NMRS data collection and gas mixture switching: Gas switching was not synchronised to the NMRS data collection. The slightly larger error bars observed between 4 and 7 minutes after onset of anoxia in the HbT, HbO₂, mean arterial blood pressure, and heart rate traces are the result of small changes in the time course of the slow hyperaemic phase.

[Figure 2](#) shows typical ³¹P spectra obtained by accumulating a total of six spectra (24 FIDs) from equivalent time points in the six anoxias from the same piglet as in [Fig. 1](#). The top trace was collected in the baseline period and the middle trace at the depth of the anoxia; the latter shows a substantial decrease in PCr and increase in P_i. The lower trace shows a ³¹P spectrum during the early phase of the hyperaemic response before pH_i has returned to baseline values. The vertical dotted line shows the chemical shift of the baseline P_i peak and is included to emphasise the acid shift of the P_i peak.

[Figure 2.](#)

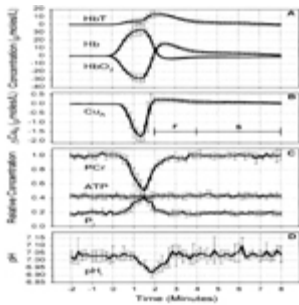


Typical ³¹P spectra from the baseline period, at the maximal depth of the anoxia, and during the postanoxia hyperaemic period from a typical piglet. PDE, phosphodiesterases; P_i, inorganic phosphate; PME, phosphomonoesters; PCr, phosphocreatine.

[Full figure and legend \(126K\)](#)

[Figure 3](#) compares the time courses of the hemoglobin signals ([Fig. 3A](#)), with HbT offset for clarity, the Cu_A signal ([Fig. 3B](#)), ³¹P signals ([Fig. 3C](#)), and pH_i ([Fig. 3D](#)) expressed as the mean and SD over all six piglets. The mean and SD of the NIR parameters from the six piglets were calculated from the mean values averaged over the six anoxias in each piglet. The patterns of cerebral desaturation and reoxygenation were the same in all piglets studied, as shown by the similarity of the NIRS changes in the pooled data ([Fig. 3](#)) compared with those from an individual piglet ([Fig. 1](#)). The larger error bars in [Fig. 3](#) compared with [Fig. 1](#) show that interpiglet variation was much greater than the intrapiglet variation.

[Figure 3.](#)



Changes in total hemoglobin (HbT), oxyhemoglobin (HbO₂), and deoxyhemoglobin (Hb) (A), oxidation state of the Cu_A centre of cytochrome oxidase (B), phosphorus metabolites (C), and intracellular pH (D) expressed as mean and SD calculated from the averaged anoxias of all six piglets. In the top panel, HbT has been offset for clarity.

[Full figure and legend \(371K\)](#)

The onset of anoxia leads to a simultaneous fall in PCr and rise in P_i (Fig. 3C). However, there is a delay between the onset of anoxia and changes in PCr and P_i. After anoxia, PCr rapidly increased to ~80% of baseline values, which corresponded to cerebral reoxygenation and the rapid reoxidation of the Cu_A centre of cytochrome oxidase. The PCr then slowly returned to baseline between 2 and 4 minutes after onset of anoxia, which corresponds to the fast phase of the hyperaemia marked as F in Fig. 3. Similar changes were observed in P_i, but the signal-to-noise ratio was lower than that of PCr. To within the error of the measurement, no change in ATP was observed. During the rapid phase of hyperaemia, the hyperoxidation of the Cu_A signal reached a maximum of 0.23 ± 0.08 $\mu\text{mol/L}$ and was significantly different from 0.0 ($P < 0.001$).

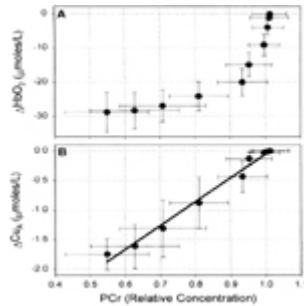
Baseline pH_i was $\sim 7.03 \pm 0.03$, and there was no significant change ($P < 0.05$) until 70 seconds after the onset of anoxia, at which point it rapidly decreased to a minimum of 6.92 ± 0.03 at 20 seconds after reoxygenation. It then rapidly returned to baseline by 3 minutes after onset of anoxia, that is, during the fast phase of hyperaemia.

The early fall in mean arterial blood pressure was observed only in two piglets (Fig. 1), and the mean value over the six piglets was observed to rise during this period. The bradycardia just before reoxygenation was observed in all piglets, with the heart rate falling to a minimum of 58 ± 6 beats/min in one piglet. The mean value over the six piglets fell from a baseline value of 182 ± 16 to 102 ± 47 beats/min and mean arterial blood pressure fell to only 48.3 ± 5.0 mm Hg, which was close to the baseline value (49.7 ± 5.1 mm Hg) during this period of bradycardia.

To emphasise the relative timings of changes in HbO₂ and Cu_A with respect to PCr, the change in HbO₂ (top) and change in Cu_A (bottom) are plotted against relative PCr concentration (baseline = 1.0) during the onset of the anoxia in Fig. 4. The line on the bottom panel of Fig. 4 is a linear regression and is included as a guide for the eye. Figure 4 clearly shows that there was a significant fall in HbO₂ before any change in PCr and

that the Cu_A signal changed coincidentally with the fall in PCr. Although the first significant ($P < 0.05$) reduction in the Cu_A centre of cytochrome oxidase occurred at 30 seconds, the change in PCr did not gain significance until 50 seconds after the onset of anoxia, probably due to the lower signal-to-noise ratio on the PCr signal compared with the Cu_A signal.

Figure 4.

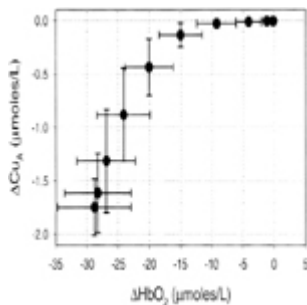


Change in oxyhemoglobin (HbO_2) (**A**) and change in Cu_A (**B**) plotted against phosphocreatine (PCr) concentration during the onset of anoxia. Results are expressed as mean \pm SD calculated over the averaged anoxias from all six piglets. The PCr is expressed as fractional concentration of baseline PCr. The line on the lower panel is a linear regression and included as a guide for the eye.

[Full figure and legend \(164K\)](#)

Figure 5 plots the change in the oxidation state of the Cu_A centre of cytochrome oxidase against the change in HbO_2 during the onset of anoxia. The first significant fall in Cu_A occurs when HbO_2 has fallen by $15.0 \pm 3.4 \mu\text{mol/L}$. The figure shows that HbO_2 can be decreased by small amounts from a baseline value without affecting the oxidation state of the Cu_A centre of cytochrome oxidase.

Figure 5.



Change in the oxidation state of the Cu_A centre of cytochrome oxidase plotted against oxyhemoglobin (HbO_2) during the onset of anoxia. Results are expressed as mean \pm SD calculated over the averaged anoxias from all six piglets.

[Full figure and legend \(95K\)](#)

[Top of page](#)

DISCUSSION

For the technique of summing NMRS spectra from corresponding time points in each anoxia to provide reliable data, it is necessary to show that the transient anoxias were highly repeatable. The results from [Table 1](#) show that, except for small changes in plasma glucose and lactate concentrations, the systemic physiological parameters did not vary significantly between each anoxia. Plasma lactate was found to increase incrementally and significantly with each anoxia from a baseline figure of 1.5 to 2.5 mmol/L before the last anoxia, but these changes were probably systemic and not cerebral in origin and are relatively small. As the blood-brain barrier is only semipermeable to lactate ([Pardridge, 1983](#)) and intracellular pH remained constant, it is unlikely that cerebral metabolism was affected. In addition, [Fig. 1](#) shows that the NIRS parameters, mean arterial blood pressure, and heart rate were highly reproducible over the course of the anoxias in each piglet, and therefore the method of summing ^{31}P FIDs over six consecutive anoxias is a valid method to increase the signal-to-noise ratio of the ^{31}P data.

The Cu_A centre of cytochrome oxidase is located on the cytosolic side of the enzyme, far from the binuclear centre where oxygen is reduced to water but close to the cytochrome c binding site ([Rich et al., 1988](#); [Iwata et al., 1995](#); [Tsukihara et al., 1995](#)). *In vitro* studies on mitochondria have shown that, in coupled turnover, the Cu_A centre of cytochrome oxidase is in redox equilibrium with cytochrome c ([Morgan and Wikström, 1991](#)), and therefore their redox potentials will be the same, albeit with the Cu_A centre slightly more reduced because its midpoint potential is slightly more positive than cytochrome c.

The results from [Fig. 3](#) and [Fig. 4](#) clearly show that there is a considerable delay between the onset of anoxia and a reduction in the cytosolic phosphorylation potential, as indicated by a fall and rise in PCr and P_i , respectively. During this period, oxygen tension at the cellular level will be falling, but the mitochondrial electrochemical potential remains constant (see [Eq. 2](#)). Therefore, either the redox states of NADH and cytochrome c do not change or their redox potentials change by equal amounts ([Eq. 1](#)). Although the ^{31}P data alone cannot provide unequivocal evidence that the redox states are not changing during this period, *in vitro* studies suggest that they do not change in parallel: In isolated mitochondria, cytochrome c begins to reduce at higher oxygen tension than NADH ([Sugano et al., 1974](#)), and in cultured kidney cells, there is little change in the redox potential of NADH at oxygen tensions that reduce cytochrome c ([Wilson et al., 1977](#)).

If it is assumed that the redox potential of NADH is fixed by the reactions of the tricarboxylic acid cycle at nonlimiting oxygen tension, then cytochrome c and Cu_A should become more reduced as the phosphorylation potential decreases. This is exactly the behaviour observed in [Fig. 3](#) and [Fig. 4](#), in which the reduction of the Cu_A signal coincides with the fall in PCr concentration, and is exactly the behaviour observed in neuroblastoma cells ([Wilson et al., 1979](#)), in which cytochrome c redox state and ^{31}P

metabolites were measured simultaneously at low oxygen tension. This is convincing evidence that the delay between the onset of anoxia and the reduction of the Cu_A signal and the relationship between HbO₂ and Cu_A, as shown in [Fig. 5](#), are not artefactual in origin but that, as measured by this system and under these conditions, changes in the Cu_A signal accurately reflect changes in the oxidation state of the Cu_A centre of cytochrome oxidase.

Once the ATP generated by glycolysis has been hydrolysed, glycolysis is a proton-generating system. These protons can either be removed from the cytosol by conversion of pyruvate to lactic acid and then exported or be metabolised to water in the mitochondria. At normoxia, the producing and consuming reactions occur at equal rates and pH homeostasis is achieved. During anoxia, when oxygen consumption is inhibited and glycolysis is expected to be stimulated, the production of hydrogen ions will exceed consumption and will lead to the acidification of the intracellular space. However, the exact point at which oxygen consumption falls is difficult to determine from changes in intracellular pH because physicochemical pH buffering would tend to mask small changes in net hydrogen ion production and also hypoxia-induced increases in CBF, which would tend to wash out CO₂ and lead to a compensatory alkalinisation of the intracellular space. In addition, even at constant CMRO₂, a fall in the phosphorylation potential is expected to increase glycolysis above baseline values, leading to a slow accumulation of lactate because glycolysis is stimulated by ADP and inhibited by ATP.

However, examination of [Fig. 3](#) shows that there is a very rapid acidification of the intracellular space, which is further delayed from the fall in PCr. This rapid acidification may well represent the point at which low oxygen tension inhibits CMRO₂, resulting in the rapid intracellular accumulation of pyruvate and lactate. This is consistent with results from the adult rat showing that, during the onset of hypoxaemia, PCr concentration falls before there is a reduction in CMRO₂ ([Norberg and Siesjö, 1975](#)). Therefore, this study would suggest that the Cu_A centre reduces during hypoxaemia at oxygen tensions that affect the phosphorylation potential but do not limit oxygen consumption.

The sequence of events during the onset of anoxia can now be determined. As arterial oxygen tension falls, initially there are no changes in phosphorylation potential and redox state of the electron transport chain until oxygen tension at the mitochondria falls to a critical value. At this critical value, there is a coincidental reduction of the electron transport chain and fall in the phosphorylation potential, but flux through the electron transport chain and oxygen consumption are not affected substantially. As PaO₂ continues to fall, there is a continuous reduction in the phosphorylation potential and reduction in the Cu_A centre of cytochrome oxidase until a second critical value is reached at which oxygen consumption is inhibited. These critical values refer to mitochondrial oxygen tension, and *in vivo* the actual mitochondrial response to hypoxaemia will be broadened by the presence of the considerable heterogeneity that has been observed in the microcirculation ([Hudetz, 1997](#)) and in tissue oxygen tension measured with microelectrodes ([Lubbers et al., 1994](#)) and the heterogeneity in mitochondria themselves ([Somnewald et al., 1998](#)).

In this study, ATP concentration did not change during the anoxia, although there is evidence that $CMRO_2$ was inhibited. Similar results were observed in adult cats in which changes in ATP concentration were not observed with hypoxia ($PaO_2 \approx 20$ mm Hg) but only when hypoxia was combined with ischaemia ([Gyulai et al., 1987](#)). In the short term, the phosphorylation potential may be prevented from falling to very low values by the stimulation of glycolysis and residual oxygen consumption over the brief period of anoxia. Once oxygen tension has fallen to a level sufficient to inhibit oxygen consumption, it is expected that components of the electron transport chain, particularly cytochrome c and Cu_A , would become almost fully reduced. Experience with performing anoxias in the piglet has shown that extending the period of anoxia does not produce a substantial further reduction in the Cu_A centre of cytochrome oxidase (data not shown), which would suggest that the Cu_A centre is almost fully reduced immediately before reoxygenation in [Fig. 1](#). During extended periods of hypoxia, when circulatory failure can occur, leading to relative ischaemia, the phosphorylation potential and PCr levels would be expected to fall to much lower levels without a further change in the Cu_A redox state. In this case, the response of the Cu_A oxidation state to PCr at low PCr concentration would become nonlinear, leading to a poorer correlation between Cu_A and PCr than shown in [Fig. 4](#).

The period between a fall in the reduction of Cu_A and the fall in oxygen consumption represents an area in which adaptation of the electron transport chain maintains electron flux to oxygen, albeit at lower phosphorylation potential. Although the adaptation involves the reduction of the Cu_A centre of cytochrome oxidase, whether this is part of the mechanism of adaptation or secondary to this mechanism is more likely to be determined from *in vitro* mitochondrial models in which redox states and electrochemical potential can be accurately measured and controlled rather than an *in vivo* model.

During the hyperemic period after reoxygenation, there is an increase in cerebral hemoglobin oxygenation and a hyperoxidation of the Cu_A signal above baseline. As it has been shown that the Cu_A oxidation state is independent of oxygen tension at normoxia, this hyperoxidation of the Cu_A centre cannot be the result of increased oxygen tension at the mitochondrial level. However, during this period, there is expected to be an increase in ATP utilization and oxygen consumption to reestablish cellular ion gradients depleted by the anoxic insult. An increase in ATP utilization would lead to an increase in ADP concentration and a decrease in the phosphorylation potential, as is observed during the fast hyperaemic phase in [Fig. 3](#), which corresponds to the period of hyperoxidation. Although the lower phosphorylation potential would reduce Cu_A with respect to NAD ([Eq. 1](#)), increasing the ADP concentration stimulates oxygen consumption and leads to an oxidation in NAD and cytochrome c in mitochondria ([Chance and Williams, 1956](#)). The same mechanism has been used to explain an oxidation in the Cu_A signal observed in human subjects after visual stimulation ([Heekeren et al., 1999](#)). An alternative cause of the hyperoxidation of NAD and Cu_A would be a decrease in substrate supply to the tricarboxylic acid cycle ([Chance and Williams, 1956](#)), but it is not clear why there should be a decrease in substrate supply after brief anoxia. It has been suggested that after hypoxia in hippocampal slices, glycolysis is inhibited at the hexose phosphorylation reactions due to low ATP concentration ([Schurr et al., 1997](#)), but in this study, ATP

concentration remained constant. However, the two possible mechanisms of hyperoxidation could be distinguished by the measurement of tricarboxylic acid cycle rate ([Mason et al., 1995](#)) or oxygen consumption.

It has been an implicit assumption of many authors that energy metabolism has not been compromised until there is a fall in ATP concentration or a fall in CMRO₂. However, from the perspective of bioenergetics, the phosphorylation potential is a better measure of cerebral energy state than ATP concentration or total high-energy phosphate concentration because it represents the free energy available on hydrolysis of ATP that provides the thermodynamic driving force to ensure that ATP-utilising reactions, such as the sodium/potassium pumps, proceed in the forward direction. It has been observed that disturbances in cerebral function occur at higher PaO₂ than that known to limit CMRO₂ ([Siesjö, 1978](#)) and that the electrocorticogram becomes isoelectric in adult cats when PCr falls to low levels but when there are no detectable changes in ATP ([Gyulai et al., 1987](#)). These observations and the results presented here suggest that falls in ATP concentration or CMRO₂ occur late in the hypoxic process and only when the Cu_A centre is almost fully reduced.

It has been suggested that the term "dysoxia" be used to define conditions in which oxygen availability limits metabolism, in preference to the terms "hypoxia" or "hypoxaemia," which simply refer to low oxygen or low arterial oxygen tension, respectively ([Connett et al., 1990](#)). In terms of energy metabolism, "dysoxia" could be defined as a fall in the phosphorylation potential rather than a fall in ATP or CMRO₂, and the results from this study suggest that the Cu_A signal from NIRS would be a good indicator of this definition of dysoxia during hypoxaemia. However, [Eq. 1](#) shows that the oxidation state of cytochrome c and the Cu_A centre of cytochrome oxidase can also be affected by activation or inhibition of the tricarboxylic acid cycle, which would lead to changes in the redox potential of NADH and parallel changes in the redox potential of Cu_A at constant electrochemical potential; such changes may occur during hypercapnia, when there is a fall in the concentration of tricarboxylic acid cycle intermediates ([Siesjö, 1978](#)).

[Top of page](#)

References

1. Buxton RB & Frank LR. (1997) A model of the coupling between cerebral blood flow and oxygen metabolism during neural stimulation. *J Cereb Blood Flow Metab* **17**: 64–72. | [PubMed](#) | [ChemPort](#) |
2. Chance B & Williams GR. (1956) The respiratory chain and oxidative phosphorylation. *Adv Enzymol* **17**: 65–134. | [ChemPort](#) |
3. Connett RJ, Honig CR, Gayeski TEJ & Brooks A. (1990) Defining hypoxia: a systems view of VO₂, glycolysis, energetics, and intracellular PO₂. *J Appl Physiol* **68**: 833–842. | [PubMed](#) | [ChemPort](#) |
4. Cooper CE, Matcher SJ, Wyatt JS, Cope M, Brown GC, Nemoto EM & Delpy DT. (1994) Near-infrared spectroscopy of the brain: relevance to

- cytochrome oxidase bioenergetics. *Biochem Soc Trans* **22**: 974–980. | [PubMed](#) | [ChemPort](#) |
5. Cooper CE, Cope M, Springett R, Amess PN, Penrice J & Tyszczuk L et al. (1999) Use of mitochondrial inhibitors to demonstrate that cytochrome oxidase near-infrared spectroscopy can measure mitochondrial dysfunction noninvasively in the brain. *J Cereb Blood Flow Metab* **19**: 27–38. | [Article](#) | [PubMed](#) | [ChemPort](#) |
 6. Elwell CE, Cope M, Kirkby D, Owen-Reece H, Cooper CE, Reynolds EOR & Delpy DT. (1994) An automated system for the measurement of the response of cerebral blood volume and blood flow to changes in arterial carbon dioxide tension using near infrared spectroscopy. *Adv Exp Med Biol* **361**: 143–155. | [PubMed](#) | [ChemPort](#) |
 7. Erecinska M, Veech RL & Wilson DF. (1974) Thermodynamic relationships between the oxidation-reduction reactions and the ATP synthesis in suspensions of isolated pigeon heart mitochondria. *Arch Biochem Biophys* **160**: 412–421. | [PubMed](#) | [ChemPort](#) |
 8. Essenpreis M, Elwell CE, Cope M, van der Zee P, Arridge SR & Delpy DT. (1993) Spectral dependence of temporal point spread functions in human tissues. *Appl Opt* **32**: 418–425.
 9. Forman NG & Wilson DF. (1982) Energetics and stoichiometry of oxidative phosphorylation from NADH to cytochrome c in isolated rat liver mitochondria. *J Biol Chem* **257**: 12908–12915. | [PubMed](#) | [ChemPort](#) |
 10. Forman NG & Wilson DF. (1983) Dependence of mitochondrial oxidative phosphorylation on activity of the adenine nucleotide translocase. *J Biol Chem* **258**: 8649–8655. | [PubMed](#) | [ChemPort](#) |
 11. Fox PT, Raichle ME, Mintun MA & Dence C. (1988) Nonoxidative glucose consumption during focal physiologic neural activity. *Science* **241**: 462–464. | [PubMed](#) | [ISI](#) | [ChemPort](#) |
 12. Greenbaum NL & Wilson DF. (1991) Role of intramitochondrial pH in the energetics and regulation of mitochondrial oxidative phosphorylation. *Biochim Biophys Acta* **1058**: 113–120. | [PubMed](#) | [ChemPort](#) |
 13. Gyulai L, Schnall M, McLaughlin AC, Leigh JS & Chance B. (1987) Simultaneous ³¹P and ¹H-nuclear magnetic resonance studies of hypoxia and ischaemia in the cat brain. *J Cereb Blood Flow Metab* **7**: 543–551. | [PubMed](#) | [ChemPort](#) |
 14. Gyulai L, Chance B, Ligeti L, McDonald G & Cone J. (1988) Correlated in vivo ³¹P-NMR and NADH fluorometric studies on gerbil brain in graded hypoxia and hyperoxia. *Am J Physiol* **254**: C699–C708. | [PubMed](#) | [ChemPort](#) |
 15. Hampson NB, Camporesi EM, Stolp BW, Moon RE, Shook JE, Griebel JA & Piantadosi CA. (1990) Cerebral oxygen availability by NIR spectroscopy during transient hypoxia in humans. *J Appl Physiol* **69**: 907–913. | [PubMed](#) | [ChemPort](#) |
 16. Heekeren HR, Kohl M, Obrig H, Wenzel R, von Pannwitz W & Matcher SJ et al. (1999) Noninvasive assessment of changes in cytochrome-c oxidase oxidation in human subjects during visual stimulation. *J Cereb Blood Flow Metab* **19**: 592–603. | [PubMed](#) | [ChemPort](#) |

17. Hoshi Y, Hazeki O, Kakihana Y & Tamura M. (1997) Redox behavior of cytochrome oxidase in the rat brain measured by near-infrared spectroscopy. *J Appl Physiol* **83**: 1842–1848. | [PubMed](#) | [ChemPort](#) |
18. Hudetz AG. (1997) Blood flow in the cerebral capillary network: a review emphasizing observations with intravital microscopy. *Microcirculation* **4**: 233–252. | [PubMed](#) | [ChemPort](#) |
19. Iwata S, Ostermeier C, Ludwig B & Michel H. (1995) Structure at 2.8Å resolution of cytochrome c oxidase from *Paracoccus denitrificans*. *Nature* **376**: 660–669. | [Article](#) | [PubMed](#) | [ISI](#) | [ChemPort](#) |
20. Kreisman NR, Sick TJ, LaManna JC & Rosenthal M. (1981) Local tissue oxygen tension-cytochrome a₃ redox relationships in rat cerebral cortex in vivo. *Brain Res* **218**: 161–174. | [Article](#) | [PubMed](#) | [ChemPort](#) |
21. Lubbers DW, Baumgartl H & Zimelka W. (1994) Heterogeneity and stability of local PO₂ distribution within the brain tissue. *Adv Exp Med Biol* **345**: 567–574. | [PubMed](#) | [ChemPort](#) |
22. Mason GF, Gruetter R, Rothman DL, Behar KL, Shulman RG & Novotny EJ. (1995) Simultaneous determination of the rates of the TCA cycle, glucose utilization, alpha-ketoglutarate/glutamate exchange, and glutamine synthesis in human brain by NMR. *J Cereb Blood Flow Metab* **15**: 12–25. | [PubMed](#) | [ChemPort](#) |
23. Matcher SJ, Cope M & Delpy DT. (1994) Use of the water-absorption spectrum to quantify tissue chromophore concentration changes in near-infrared spectroscopy. *Phys Med Biol* **39**: 177–196. | [Article](#) | [PubMed](#) | [ChemPort](#) |
24. Matcher SJ, Elwell CE, Cooper CE, Cope M & Delpy DT. (1995) Performance comparison of several published tissue near-infrared spectroscopy algorithms. *Anal Biochem* **227**: 54–68. | [Article](#) | [PubMed](#) | [ChemPort](#) |
25. Matsumoto H, Oda T, Hossain MA & Yoshimura N. (1996) Does the redox state of cytochrome aa₃ reflect brain energy level during hypoxia? Simultaneous measurements by near infrared spectrophotometry and ³¹P nuclear magnetic resonance spectroscopy. *Anesth Analg* **83**: 513–518. | [PubMed](#) | [ChemPort](#) |
26. Moon RB & Richards JH. (1973) Determination of intracellular pH by ³¹P magnetic resonance. *J Biol Chem* **48**: 7276–7278.
27. Morgan JE & Wikström M. (1991) Steady-state redox behaviour of cytochrome c, cytochrome a, and Cu_A of cytochrome oxidase in intact rat liver mitochondria. *Biochemistry* **30**: 984–958.
28. Morris P & Freeman R. (1978) Selective excitation in Fourier transform nuclear magnetic resonance. *J Magn Res Imag* **29**: 433–462.
29. Nishiki K, Erecinska M & Wilson DF. (1978) Energy relationships between cytosolic metabolism and mitochondrial respiration in rat heart. *Am J Physiol* **234**: C73–C81. | [PubMed](#) | [ChemPort](#) |
30. Norberg K & Siesjö BK. (1975) Cerebral metabolism in hypoxic hypoxia I. Pattern of activation of glycolysis: a re-evaluation. *Brain Res* **86**: 31–44. | [Article](#) | [PubMed](#) | [ChemPort](#) |
31. Pardridge W. (1983) Brain metabolism: a perspective from the blood-brain barrier. *Physiol Rev* **63**: 1481–1528. | [PubMed](#) | [ChemPort](#) |

32. Rich PR, West IC & Mitchell P. (1988) The location of Cu_A in mammalian cytochrome c oxidase. *FEBS Lett* **233**: 25–30. | [Article](#) | [PubMed](#) | [ChemPort](#) |
33. Schurr A, Payne RS, Miller JJ & Rigor BM. (1997) Brain lactate, not glucose, fuels the recovery of synaptic function from hypoxia upon reoxygenation: an in vitro study. *Brain Res* **744**: 105–111. | [Article](#) | [PubMed](#) | [ChemPort](#) |
34. Siesjö BK. 1978 Brain energy metabolism Chichester: Wiley.
35. Sonnewald U, Hertz L & Schousboe A. (1998) Mitochondrial heterogeneity in the brain at the cellular level. *J Cereb Blood Flow Metab* **18**: 231–237. | [Article](#) | [PubMed](#) | [ChemPort](#) |
36. Sugano T, Oshino N & Chance B. (1974) Mitochondrial functions under hypoxic conditions. The steady states of cytochrome c reduction and of energy metabolism. *Biochim Biophys Acta* **347**: 340–358. | [PubMed](#) | [ChemPort](#) |
37. Tsuji M, Naruse H, Volpe J & Holtzman D. (1995) Reduction of cytochrome aa3 measured by near-infrared spectroscopy predicts cerebral energy loss in hypoxic piglets. *Pediatr Res* **37**: 253–259. | [PubMed](#) | [ChemPort](#) |
38. Tsukihara T, Aoyama H, Yamashita E, Tomizaki T, Yamaguchi H & Shinzawa-Itoh K et al. (1995) Structure of metal sites of oxidized bovine heart cytochrome c oxidase at 2.8Å. *Science* **269**: 1069–1074. | [PubMed](#) | [ISI](#) | [ChemPort](#) |
39. Wang H & Oster G. (1998) Energy transduction in the F₁ motor of ATP synthase. *Nature* **396**: 279–282. | [Article](#) | [PubMed](#) | [ISI](#) | [ChemPort](#) |
40. Wilson DF, Erecinska M, Drown C & Silver IA. (1977) Effects of oxygen tension on cellular energetics. *Am J Physiol* **233**: C135–C140. | [PubMed](#) | [ChemPort](#) |
41. Wilson DF, Erecinska M, Drown C & Silver IA. (1979) The oxygen dependence of cellular energy metabolism. *Arch Biochem Biophys* **195**: 485–493. | [Article](#) | [PubMed](#) | [ChemPort](#) |